Entangled Optical Vortex Links

J. Romero,[1,2] J. Leach,[1] B. Jack,[1] M. R. Dennis,[3] S. Franke-Arnold,[1] S. M. Barnett,[2] and M. J. Padgett[1]

[1]*School of Physics and Astronomy, SUPA, University of Glasgow, Glasgow G12 8QQ, United Kingdom*
[2]*Department of Physics, SUPA, University of Strathclyde, Glasgow G4 ONG, United Kingdom*
[3]*H. H. Wills Physics Laboratory, University of Bristol, Bristol BS8 1TL, United Kingdom*

(Received 15 June 2010; revised manuscript received 9 November 2010; published 11 March 2011)

Optical vortices are lines of phase singularity which percolate through all optical fields. We report the entanglement of linked optical vortex loops in the light produced by spontaneous parametric down-conversion. As measured by using a Bell inequality, this entanglement between topological features extends over macroscopic and finite volumes. The entanglement of photons in complex three-dimensional topological states suggests the possibility of entanglement of similar features in other quantum systems describable by complex scalar functions, such as superconductors, superfluids, and Bose-Einstein condensates.

DOI: 10.1103/PhysRevLett.106.100407 PACS numbers: 03.65.Ud, 03.67.Bg, 42.50.Dv

Most current optical experiments on entanglement use spontaneous parametric down-conversion (SPDC) as the source of correlated photon pairs. The simultaneous conservation of both energy and momentum in the SPDC process leads to various properties of the photons exhibiting quantum entanglement. For example, correlations are present in the spatial modes of the signal and idler photons [1,2] including those modes associated with orbital angular momentum (OAM) [3–5]. Eigenmodes of optical OAM have phase singularities (optical vortices) along the beam axis. These lines are zeros of the complex field amplitude.

Optical vortex lines are found throughout optical speckle, occurring between the bright speckles and seen as dark points where the singularity lines intersect the imaged plane. In three-dimensional (3D) speckle, these vortex lines form a fractal tangle, percolating through space [6], with many closed loops which are occasionally linked together [7]. Light produced by SPDC is spatially incoherent and can also be considered as an example of optical speckle [8], making this light a good candidate in which to observe topological vortex features. Here we show that quantum correlations exist between spatially separated vortex features of electromagnetic fields. Specifically, we show that links of vortex loops embedded within optical fields produced by SPDC are entangled.

The Laguerre-Gaussian (LG) set of optical modes contains axial vortex lines and hence is a convenient basis for specifying modal superpositions with linked vortex loops. These LG modes are characterized by an azimuthal phase dependence $\exp(i\ell\phi)$, giving $\ell\hbar$ as the OAM per photon [9]. The entanglement of the OAM of photons has been observed experimentally [4,10] and, more recently, has been demonstrated by violating the Bell inequality within 2D subspaces [11]. However, in this present work, the entanglement of OAM is not our primary concern but rather the entanglement of macroscopic vortex features that can be synthesized by combining LG modes, including those possessing no OAM.

The modal superpositions that form the links can be generated by using specially designed diffractive optical components (holograms). Although specified only in two dimensions, holograms determine the propagation of the whole optical field behind them. Previously, holograms have transformed the Gaussian output of a laser or single-mode fiber into a field with a pair of linked phase singularity loops (Hopf links) [12]. The same hologram that transforms a Gaussian mode into the Hopf link can be used in reverse as a measurement hologram; that is, it can be used to detect the 3D feature. In our case, this transforms a Hopf link back to the fundamental Gaussian mode which can then, and only then, be coupled into a single-mode fiber and photon detector. A single photon detection constitutes the single photon measurement of the 3D topological state.

In modal superpositions of this kind, the linked vortex lines intertwine within regions of very low optical intensity. The practical generation and observation of these topological features relies on the numerical optimization of the complex mode coefficients to separate the vortex lines by regions of higher intensity [12]. Once the optimum coefficients of the modal components in the superposition are determined, it is a simple matter to design the corresponding detection hologram.

The modal superposition to produce the vortex Hopf link is given by

$$|\Psi_{\text{Hopf link}}\rangle = 0.264|0,0\rangle - 0.628|0,1\rangle + 0.426|0,2\rangle - 0.596e^{i2\theta}|2,0\rangle, \quad (1)$$

where $|\ell, p\rangle$ denote the LG mode with p radial nodes and azimuthal index ℓ and θ defines the orientation of the Hopf link in the x-y plane. We use a pump beam of zero OAM in

 © 2011 American Physical Society

the state $|0, 0\rangle$ from which the entangled SPDC state can be written in the LG basis as

$$|\Psi_{\mathrm{SPDC}}\rangle = \sum_{p_s=0}^{\infty} \sum_{p_i=0}^{\infty} \sum_{\ell=-\infty}^{\infty} c_{-\ell,p_i}^{\ell,p_s} |\ell, p_s\rangle| - \ell, p_i\rangle, \qquad (2)$$

where $|c_{-\ell,p_i}^{\ell,p_s}|^2$ is dependent on the down-conversion process and is the probability of generating a photon pair in the $|\ell, p_s\rangle$ and $|-\ell, p_i\rangle$ states [13–15]. The state (2) has a range of different modes including the modes which comprise the superposition that could form the links. We can separate the superposition (1) into two components consisting of modes with zero and nonzero OAM ($\ell = 0$ and $\ell = 2$, respectively), if we define the state $|0, p\rangle = 0.329|0, 0\rangle - 0.782|0, 1\rangle + 0.530|0, 2\rangle$, which we get by normalizing the first three terms of (1). We can then write the Hopf link state as $|\Psi_{\mathrm{Hopf\ link}}\rangle = \alpha|0, p\rangle - \beta e^{i2\theta}|2, 0\rangle$, where $\alpha = 0.803$ and $\beta = 0.596$. We can then define our measurement states in a two-dimensional (2D) subspace. The advantage of a 2D subspace is that it lends itself to traditional tests of entanglement such as the Bell inequality [16].

At the heart of entanglement are the correlations exhibited in the bases corresponding to incompatible observables (e.g., linear and circular polarization). In a 2D state space, the concept of incompatible observables is best illustrated by a reference to a Bloch sphere where, for example, a rotation of linear polarization is equivalent to a change in phase between the constituent circular polarizations. We can cast the measurement of Hopf links similarly, in that we can have an unconventional Bloch sphere based on superposition (1). The north pole of this Bloch sphere corresponds to the weighted superposition $\alpha|0, p\rangle$, and the south pole corresponds to $\beta|2, 0\rangle$. The equatorial states of this Bloch sphere are then the Hopf links oriented at different angles, θ [see Fig. 1(a)]. To show entanglement between the Hopf links requires demonstrating that the strength of nonlocal correlations depend not only on the magnitude of the modes (the poles of the sphere) but also on their relative phases. We test this phase dependence by changing the relative angular orientations of the topological features measured in the signal and idler beams. If the observed correlations were simply and solely due to classical conservation, then the strength of the correlations would show no phase dependence. We also show the confinement of the Hopf link to a finite volume and the dependence of the entanglement on relative spatial position. To one of the holograms, we introduced lateral and axial shifts, the latter giving a Gouy phase between the modes [17]. Rather than moving any of the optical components, we apply these shifts directly by setting the phase of the modal superpositions for the hologram design.

We employ the experimental configuration shown in Fig. 2(a). A quasi-cw, mode-locked, UV pump beam at 355 nm is incident on a 3-mm-long type-I barium borate

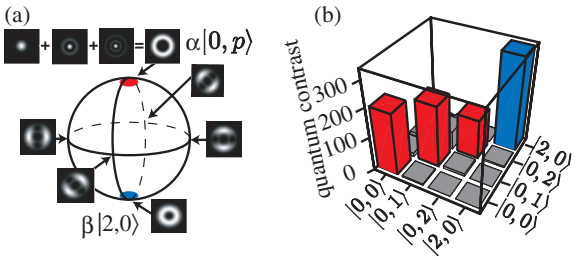

FIG. 1 (color). A Bloch sphere for Hopf links and correlations among the constituent LG modes in the state (1). (a) A Bloch sphere for the Hopf links has the state $\alpha|0, p\rangle$ (with constant phase and a small nonzero on-axis intensity) and $\beta|2, 0\rangle$ (or $\beta|-2, 0\rangle$) at the poles. The equatorial states correspond to the Hopf links. (b) Red bars show the correlation between the $\ell = 0$ states that make up $|0, p\rangle$ (north pole), and the blue bar corresponds to the correlation between the $\ell = 2$ and $\ell = -2$ states (south pole).

(BBO) crystal. The crystal is oriented in a collinear geometry with the down-converted 710 nm signal and idler photons both incident on the same beam splitter. The exit face of the crystal is imaged to separate spatial light modulators (SLMs). The SLMs are used to display the measurement holograms which specify the links we aim to detect. These SLMs are reimaged to the input facets of single-mode fibers which are themselves coupled to avalanche photodiodes for single photon detection. The coincidence count rate from the two detectors is recorded as the holograms displayed on the SLMs are updated. The SLMs that we use are phase-only modulators; however, by appropriate design of an off-axis hologram, they can generate

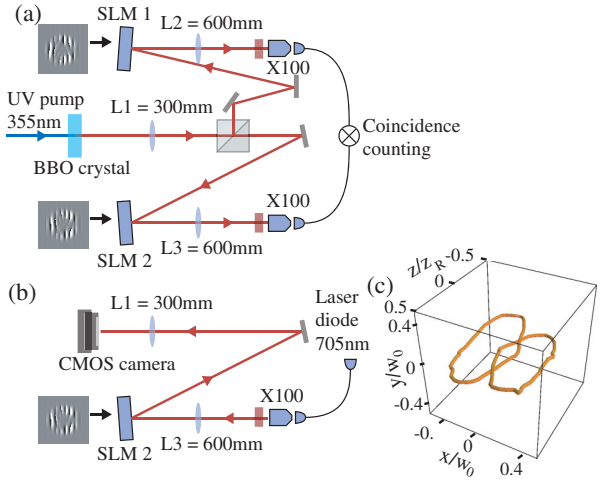

FIG. 2 (color online). Experiment scheme. (a) The topological states are measured by encoding holograms displayed on separate SLMs. (b) Using one of the arms in the same setup, we back-project through the measurement hologram to verify the topology of the field. (c) The recovered topology is a Hopf link; x, y, and z refer to shifts in the x, y, and z directions, respectively. Dimensions have been normalized by the beam waist w_0 and Rayleigh range z_R.

or detect any modal superposition, even those involving a modulation in intensity [18].

We confirmed that this hologram indeed generates a Hopf link by replacing one of the detectors with a laser diode sending light back to the SLM and then recovering the phase and intensity of the diffracted light field in the plane of the crystal [Fig. 2(b)] [12]. We then programmed the SLM to introduce axial displacements of the vortex positions with respect to the plane of the crystal allowing us to tomographically reconstruct the link structure as shown in Fig. 3(c).

In the image plane of the crystal, the signal and idler fields are complex conjugates of each other. This means if the photons are projected by the holograms which are encoded in states which are themselves complex conjugates of each other, the correlation between signal and idler beams should be high. The LG basis that we use to describe our topological features is an orthonormal, complete set, and consequently the correlation between any two modes of differing indices should, ideally, be zero. Before examining the correlation between the topological features themselves, we examine these measured correlations between the four LG modes that form the Hopf link [see Fig. 1(b)]. We calculate the ratio of the measured coincident rate C to that anticipated from accidental coincidences; we call this ratio the quantum contrast, and it is given by $\mathrm{QC} = C/(S_i S_s \Delta t)$, where S_i and S_s are idler and signal count rates, respectively, and Δt is the timing resolution of our coincidence counting electronics [19]. As anticipated, the correlation between any mode and its complex conjugate is high, while its correlation with all other modes is low. We note, however, that some nominally orthogonal modes have residual correlations, which arise from the finite aperture of our system. This imperfection potentially reduces the degree of the entanglement, but, as we show below, the entanglement we observe is still sufficient to violate a Bell inequality.

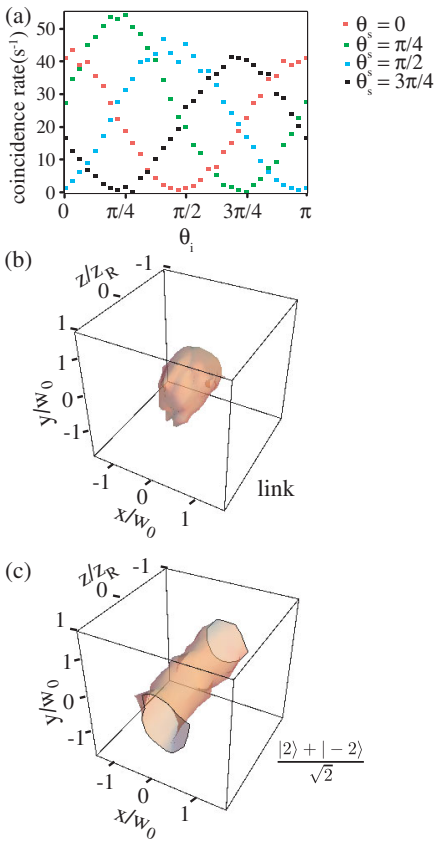

FIG. 3 (color). Experimental evidence of entanglement of topological states. (a) Coincidence curves show a phase dependence on angular orientations θ_s and θ_i from which we obtain $S = 2.72$ when the signal and idler holograms are both on the $z = 0$ plane. (b) $S = 2$ surface for a Hopf link and (c) for a simple superposition of OAM states. x, y, and z refer to shifts in the x, y, and z directions, respectively. Dimensions have been normalized by the beam waist w_0 and Rayleigh range z_R.

With the SLMs displaying holograms to measure the Hopf link and its complex conjugate, we measure the coincident count rate as a function of their angular orientations θ_s and θ_i. The sinusoidal nature of the coincidence count rates is reminiscent of the coincidence curves used to show a violation of the Bell inequality in the case of polarization-entangled photons. Indeed, the fact that our state can be written in terms of two orthogonal sets of modes means we can perform a similar analysis for our Hopf links [16]. We use the Clauser-Horne-Shimony-Holt inequality [20], which gives the Bell parameter S and is violated when $|S| > 2$. The extent to which this inequality can be violated is an indication of the degree of entanglement of a quantum system, with S taking on a value of $2\sqrt{2}$ for maximally entangled states.

Because the Hopf link contains a component with $\ell = 0$, the Hopf link and its complex conjugate are not completely orthogonal; hence, the coincidence rate should not fall to exactly zero as would be the case for the maximally entangled case [21]. We obtain lower minima in our coincidence curves, and this is a consequence of the interference arising from modes that are ideally orthogonal [i.e., the off-diagonal modes in Fig. 1(b)] but experimentally give residual coincidence counts. Figure 3(a) shows a sample set of coincidence curves used to calculate S from four different orientations of the signal hologram as the orientation of the idler hologram is varied from 0 to π (corresponding to a phase change between the $\alpha|0, p\rangle$ and $\beta|2, 0\rangle$ of 0 to $2\theta_i = 2\pi$). The near sinusoidal shape is an indication that we largely remain in a 2D state space. Following Ref. [22], we obtain a Shannon dimensionality of 1.92. We measure S to be 2.72 ± 0.012 when the signal and idler holograms are laterally and axially aligned, greater than the classical limit of 2, thereby demonstrating that the Hopf links we measure in the down-converted fields are indeed entangled.

The unique aspect of these entangled states is that the topological feature is spatially localized in 3D. We show

this by measuring S as a function of both lateral and axial displacements of the measured links and compare this volumetric scan to that obtained for the simple superposition of $|\pm\ell\rangle$ OAM states used to show the entanglement of OAM [Figs. 3(b) and 3(c)]. In this latter case we use a superposition of $\ell = \pm 2$, measuring the count rate and obtaining S as a function of lateral and axial displacement. As might be expected, for pure OAM entanglement we see that the value of S falls for lateral displacement, yet the structural stability of the mode means that S does not fall with axial displacement. By contrast, we see that the volume over which the Hopf link violates the Clauser-Horne-Shimony-Holt inequality ($S > 2$) is bounded in both the lateral and axial directions to a size similar to that of the experimentally recovered Hopf link [Fig. 2(c)].

The SLMs that we use have a diffraction efficiency of about 60%. We are using off-axis holograms, meaning that any phase noise in the SLM will affect only the diffraction efficiency and not the phase of the measured state, which is instead set by the spatial form of the hologram. We note that the topology of the Hopf link is recreated in the back-projection experiment, inferring that these are the states we measure. In any event, the fact that we violate the Bell inequality is an unambiguous demonstration of quantum entanglement and demonstrates that we are not significantly constrained by the limitations of our SLMs.

Whereas earlier work in quantum entanglement has concentrated on two separated point properties of the field (e.g., polarization) or two field cross sections (e.g., OAM), our present work shows a signature of entanglement between two separated and finite volumes. Specifically, our measurements relate to topological features of the scalar electromagnetic field. Similar wave descriptions are equally applicable to various physical situations involving cold atoms, superfluids, and other condensed matter systems. The existence of vortex lines and related topological features in these systems is an area of intense theoretical and experimental investigation [23–25]. We conjecture that the quantum entanglement of topological features of vortex lines may extend to cover these other system types. The transfer of the topological vortex states from light to a Bose-Einstein condensate [24,26] may be a route to the preparation of macroscopically entangled topological states.

A further point is that, since topological states are usually robust to perturbation [27], they may offer a route to increasing the stability of the entangled state. Indeed, the stability of topology has, in two-dimensional physics, led to the field of topological quantum computation [28]. The degree to which three-dimensional vortex topological features are stable or not depends upon the details of the physical system in which they occur. For example, if vortex lines are subject to a repulsive force between them, as can be the case in a nonlinear media [29], this acts to stabilize their topology. Unfortunately, for light beams in free space this is not the case, and therefore topology is unlikely to mitigate, for example, the effect of atmospheric turbulence. However, other physical systems may not be limited in this way.

We thank the United Kingdom EPSRC, Leverhulme Trust, Future and Emerging Technologies (FET) program (HIDEAS No. FP7-ICT-221906), and Hamamatsu. M. R. D. thanks the Royal Society. S. M. B. and M. J. P. thank the Royal Society and the Wolfson Foundation.

[1] D. Klyshko, Phys. Lett. A **132**, 299 (1988).
[2] K. Wagner *et al.*, Science **321**, 541 (2008).
[3] A. Mair *et al.*, Nature (London) **412**, 313 (2001).
[4] N. K. Langford *et al.*, Phys. Rev. Lett. **93**, 053601 (2004).
[5] M. Lassen, G. Leuchs, and U. L. Andersen, Phys. Rev. Lett. **102**, 163602 (2009).
[6] K. O'Holleran *et al.*, Phys. Rev. Lett. **100**, 53902 (2008).
[7] K. O'Holleran, M. R. Dennis, and M. J. Padgett, Phys. Rev. Lett. **102**, 143902 (2009).
[8] R. Ghosh *et al.*, Phys. Rev. A **34**, 3962 (1986).
[9] L. Allen *et al.*, Phys. Rev. A **45**, 8185 (1992).
[10] A. Vaziri, G. Weihs, and A. Zeilinger, Phys. Rev. Lett. **89**, 240401 (2002).
[11] J. Leach *et al.*, Opt. Express **17**, 8287 (2009).
[12] M. R. Dennis *et al.*, Nature Phys. **6**, 118 (2010).
[13] J. Torres *et al.*, Phys. Rev. A **67**, 052313 (2003).
[14] C. K. Law and J. H. Eberly, Phys. Rev. Lett. **92**, 127903 (2004).
[15] A. Yao, arXiv:1012.5021.
[16] J. Bell, *Speakable and Unspeakable in Quantum Mechanics* (Cambridge University Press, Cambridge, England, 1987).
[17] D. Kawase *et al.*, Phys. Rev. Lett. **101**, 050501 (2008).
[18] B. Jack *et al.*, Phys. Rev. A **81**, 043844 (2010).
[19] D. Burnham and D. Weinberg, Phys. Rev. Lett. **25**, 84 (1970).
[20] J. F. Clauser *et al.*, Phys. Rev. Lett. **23**, 880 (1969).
[21] S. Phoenix and S. Barnett, Phys. Lett. A **167**, 233 (1992).
[22] J. B. Pors *et al.*, Phys. Rev. Lett. **101**, 120502 (2008).
[23] C. van der Wal *et al.*, Science **290**, 773 (2000).
[24] N. LoGullo *et al.*, Phys. Rev. A **81**, 053625 (2010).
[25] O. Auslaender *et al.*, Nature Phys. **5**, 35 (2008).
[26] K. Kapale and J. Dowling, Phys. Rev. Lett. **95**, 173601 (2005).
[27] R. Pugatch *et al.*, Phys. Rev. Lett. **98**, 203601 (2007).
[28] C. Nayak *et al.*, Rev. Mod. Phys. **80**, 1083 (2008).
[29] W. Firth and D. Skyrabin Phys. Rev. Lett. **79**, 2450 (1997).